

Dynamics of chevron structure formation

A. N. Shalaginov,* L. D. Hazelwood, and T. J. Sluckin

*Southampton Liquid Crystal Institute and Faculty of Mathematical Studies, University of Southampton,
Southampton SO17 1BJ, United Kingdom*

(Received 23 April 1998)

The natural structure for smectic-*A* liquid crystals arranged in a sample with homogeneous boundary conditions is the so-called bookshelf structure with uniform layers perpendicular to the sample cell plane. However, this structure often deforms into the so-called chevron structure when the sample is cooled. This deformation is usually thought to result from the mismatch between bulk and surface layer thicknesses. In this paper we study the dynamics of chevron formation. Two possible scenarios are envisaged. In one of these there is strong coupling between layer deformation and fluid flow, and in the other the fluid essentially does not move. In this paper we examine the first scenario, leaving the second, slower relaxation mode for another paper. Analytic solutions are found for near-critical deformations, and numerical solutions are found beyond the critical regime. [S1063-651X(98)06912-8]

PACS number(s): 61.30.Cz, 42.79.Kr, 64.70.Md, 83.70.Jr

I. INTRODUCTION

There have been a number of recent studies of smectic liquid crystals confined between parallel boundaries and subject to homogeneous boundary conditions. The natural expected smectic texture in this case is the so-called bookshelf structure, in which the smectic layers are arranged in a stack with the layer normal parallel to an easy direction in the plane of the walls. However, this bookshelf structure occurs only rarely, and more often the bookshelf texture spontaneously deforms into the so-called chevron structure in which the layer edges at the wall are not shifted, but the layers are tilted, in the same sense at each wall, and meet in the center of the sample at the so-called chevron tip. An understanding of the chevron structure is of considerable importance in the development of surface-stabilized ferroelectric smectic display devices.

The chevron structure was observed first in a ferroelectric smectic-*C* material by Rieker *et al.* [1], and it is in this area that the practical importance of the problem lies. This chevron structure has been the focus of a good deal of theoretical work in order to disentangle the principles underlying optical switching in ferroelectric smectic-*C* cells [2].

However, the chevron structure has also been observed in a Sm-*A* material [3,4], and this rather simpler system provides a good testing ground for theories of chevron formation. Theories of the statics of the chevron structure in the Sm-*A* phase have been proposed by Limat and Prost [5] and examined in slightly more detail by Kralj and Sluckin [6]. In this paper we extend these studies to provide a theory of the dynamics of chevron formation.

The crucial idea behind theories of chevron structure [5–7] is that the layer tilt is supposed to arise because of mismatch between the natural—thermodynamically stable—smectic layer thickness and that imposed by layer pinning at the cell surface. This mismatch is a result of a competition

between the sample history (which provides a fixed layer surface-induced thickness) and thermodynamics, which imposes an (albeit weak) temperature-dependent bulk layer thickness.

The governing parameter for this mismatch is the layer strain $\epsilon = 1 - q_B/q$, where q_B, q are, respectively, the wave vectors associated with the bulk and surface layer thicknesses. This layer strain is the fractional difference between the intrinsic smectic layer thickness and that imposed on the system by the surface (or equivalently by the previous history of the sample). The layer distortion occurs above a critical value $\epsilon_c = 4\pi^2 K/BL^2$, where K and B are the elastic constants associated with layer bending and compression, and L is the cell thickness.

In this paper we shall assume, following other workers, that there are no defects in the smectic structure within the cell. We shall also suppose that the bulk smectic provides an imprint on the surface in a such a way that the surface has a memory of the layer structure above it. However, notwithstanding the existence of experimental evidence for such surface memory [8], the present study gives some support to the view that this assumption is stronger than necessary. Rather we believe that the absence of defects, or, equivalently, the conservation of layers, combined with the no-slip velocity condition and the extremely slow time scale of the nonequilibrium layer drift through the smectic fluid, combine to impose the chevron structure.

The formation of the chevron structure for strains larger than critical involves two sequential processes. First, thermal fluctuations provide small departures from the original bookshelf structure. These fluctuations are then amplified until the new chevron structure emerges. We study the second of these processes, which is governed by Sm-*A* hydrodynamics. We shall use the standard theory of Sm-*A* hydrodynamics, as described by de Gennes and Prost [9] or Chaikin and Lubensky [10]. The crucial change as compared to these expositions will be in the form of the free energy functional.

The plan of the paper is as follows. In Sec. II we shall recap on previous work on the statics of the chevron state. We introduce the free energy functional underlying our

*Permanent address: Department of Physics, University of St. Petersburg, St. Petersburg 198904, Russia.

study, and explain how minimizing this functional leads naturally to chevron formation. In Sec. III we introduce the hydrodynamic equations that govern Sm-A motion. In Sec. IV we solve the equations in the case for which layer-fluid flow coupling is the dominant process. The alternative scenario in which flow is suppressed will be treated in a subsequent paper [16]. Finally in Sec. V we make some concluding remarks.

II. STATICS

A. Free energy

The natural order parameter in the Sm-A phase is the complex quantity $\psi = \eta \exp iW(\mathbf{r}, t)$ [6,9]. The magnitude of this order parameter η provides a measure of the magnitude of the smectic density wave, whereas the phase W yields information about the position of the layers. We here discuss a system in which the smectic order parameter has no singularities, and we shall therefore suppose that the quantity η is unaffected through the process of chevron formation.

In a uniform stationary system the phase can be described by the relation $W(\mathbf{r}) = q_B z$, where \mathbf{e}_z is the layer normal, and the layer spacing $d_B = 2\pi/q_B$. In fact, the transformation $W \rightarrow -W$; $\psi \rightarrow \psi^*$ leaves the system unchanged, and this is important in constructing the free energy. The free energy contains compression terms that specify the favored layer thickness, and bending terms that favor a director that remains uniform. The free energy must be invariant with respect to translating the smectic layers by arbitrary amounts, and can therefore only depend on gradients of W , and not on W itself, except at surfaces. Although some free energy formulations explicitly separate the nematic director $\hat{\mathbf{n}}$ and the layer normal $\hat{\mathbf{a}} = \nabla W / |\nabla W|$, we shall remark that these variables are usually strongly coupled, with a relaxation time of order 10^{-7} sec [11], and we shall simply suppose that $\hat{\mathbf{a}} = \hat{\mathbf{n}}$. We use the free energy functional [12]

$$F = \int d^3r f(\mathbf{r}), \quad (1)$$

where the free energy density is given by

$$f(\mathbf{r}) = \frac{1}{8} B [q_B^{-2} (\nabla W)^2 - 1]^2 + \frac{1}{2} K q_B^{-2} (\nabla^2 W)^2. \quad (2)$$

In this equation K and B have their usual significance of Frank bend elastic constant and layer compressibility, respectively. The formulation explicitly allows for the $W \rightarrow -W$ symmetry, and thus yields equivalent minima of $W = \pm q_B z$, both of which describe a stack of smectic layers perpendicular to the z axis. The interesting inevitable consequence of this symmetry is the existence of the $(\nabla W)^4$ term, which has crucial significance in stabilizing the free energy functional. This term may otherwise be thought of coming from the term coupling the director with the smectic order parameter, after the explicit director dependence has been integrated out.

We now make contact with the familiar elastic formulation of the Sm-A free energy. Deviations from equilibrium can be described in terms of the layer displacement u , where

$$W(x, z, t) = q[z - u(x, z, t)]. \quad (3)$$

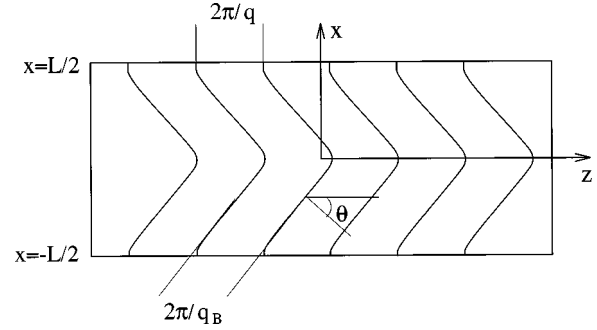


FIG. 1. The chevron structure in a cell of thickness L , showing mismatch between surface wave vector $q = 2\pi/a_B$ and bulk wave vector $q_B = 2\pi/a$, with x axis and z axis marked.

If $q = q_B$ the elastic energy can then be expressed, in quadratic order, as

$$f = \frac{1}{2} B \left(\frac{du}{dz} \right)^2 + \frac{1}{2} K (u_{xx})^2, \quad (4)$$

which is the usual smectic expression for the elastic energy. In all subsequent equations we shall consider $u(\mathbf{r}, t)$ as the dynamical variable.

We show the chevron geometry in Fig. 1. In the case of a static uniform deformation there is no y dependence. The layer is tilted with respect to its original direction by a small angle $\theta \approx u_x$, and $W = q(z - u(x))$. Note that $q \neq q_B$ here; we consider displacements from a configuration with the imposed rather than the bulk layering. Implicitly we have quenched from a sample in which q was the bulk wave number and the cell had equilibrated.

We now substitute the ansatz (3) into Eq. (2). Dropping higher-order terms in ϵ yields the Limat-Prost formulation [5] of the chevron problem:

$$F = \frac{1}{2} \int d^3r \left[B \left(\frac{1}{2} \theta^2 - \epsilon \right)^2 + K \left(\frac{\partial \theta}{\partial x} \right)^2 \right], \quad (5)$$

where we have used the approximation $1 - q^2/q_B^2 \approx 2\epsilon$.

The equations for static equilibrium are

$$\frac{\delta F}{\delta u} = -\frac{d}{dx} \frac{\delta F}{\delta \theta} = 0. \quad (6)$$

Finally in this section, we make an observation about the procedure for finding the equilibrium layer profile, whose relevance will become more obvious when discussing the dynamics. Varying the free energy with respect to the variable θ gives Euler-Lagrange equations that explicitly include the layer strain ϵ . By contrast, varying the free energy with respect to the layer displacement $u(x)$ gives rise to an Euler-Lagrange equation that does not include the layer strain; the layer strain only enters the solution in the first integral of this equation.

B. Stability analysis

It will be useful at this stage to remind the reader of the detailed arguments leading to the static chevron structure. The Hamiltonian, Eq. (5) above, is minimized for $\theta = \pm \theta_0$

$= \pm \sqrt{2\epsilon}$. These values of θ , corresponding to leftward or rightward layer tilts with respect to the original bookshelf geometry, are the only values of θ consistent with the imposed periodic geometry that preserve the thermodynamically imposed layer spacing. The problem with either of these solutions is that they involve uniformly tilted layers, whereas the boundary conditions demand that the layer displacement at each surface of the cell be zero. The surface Hamiltonian, in contrast to the bulk Hamiltonian, is sensitive to the absolute value of the phase W ! Thus the uniform solutions $\pm \theta_0$ do not preserve the surface layer structure. The simplest structure that does preserve the surface layer structure is one for which $\theta = +\theta_0$ in the top half of the cell, and $\theta = -\theta_0$ in the bottom half of the cell (or vice versa), while close to the cell walls and in the middle of the cell, there is a region of intermediate behavior. The region close to the cell walls depends on the detailed boundary conditions involved. The region in the center, of thickness $\sim \lambda_{ch} = (K/\epsilon B)^{1/2}$, is the so-called chevron tip; in this region the tilt in the layers more or less abruptly reverses.

Now, in order that the system may take advantage of the free energy reduction implied by the layer tilt θ_0 , it must overcome the pain of bending over a length scale L . This it will not be able to do unless the chevron tip length scale λ is shorter than the cell size L . This may be seen formally by examining the perturbation to the bookshelf free energy induced by a small angle $\theta(x)$ at quadratic order:

$$\Delta F = \int dy dz \int_{L/2}^{L/2} dx \frac{1}{2} \left[-\epsilon B \theta^2 + K \left(\frac{d\theta}{dx} \right)^2 \right]. \quad (7)$$

For simplicity we suppose that $\theta=0$ on the boundaries. The fluctuation responsible for the initiation of the chevron phase is

$$u_0(x) = u_0 [1 + \cos(2\pi x/L)] \quad (8)$$

or

$$\theta = \vartheta_0 \sin(2\pi x/L). \quad (9)$$

The quantity ΔF is positive, and thus the formation of a chevron phase is disfavored, if

$$-B\epsilon + \frac{4\pi^2}{L^2} K > 0. \quad (10)$$

This gives a condition for the critical strain ϵ_c :

$$\epsilon < \epsilon_c = \frac{4\pi^2 K}{BL^2}, \quad (11)$$

and an equivalent condition for the relationship between the cell width L and the critical length scale λ_{ch} ,

$$\lambda_{ch} \geq \frac{L}{2\pi}. \quad (12)$$

Normally, ϵ and ϵ_c are small values, so it is useful to introduce a dimensionless quantity governing chevron formations. This is the chevron number σ [6],

$$\sigma = \frac{\epsilon}{\epsilon_c} = \frac{BL^2 \epsilon}{4\pi^2 K}, \quad (13)$$

which allows one to measure ϵ in terms of the critical strain.

An equivalent formulation of this stability criterion is that the eigenvalues C of the equation

$$-B\epsilon u_{xx} + K u_{xxxx} = C u \quad (14)$$

($u=0, u_x=0$ on the boundaries) should be all negative.

It is instructive to estimate the magnitude of the fluctuations in the bookshelf structure due to the critical mode given by Eq. (9). The energy cost associated with a fluctuation of the Hamiltonian, Eq. (4), is equal to $VB(\epsilon_c - \epsilon) \vartheta_0^2/4$, where V is the cell volume. Using the equipartition theorem, the mean-square fluctuation can be found to be

$$\langle \vartheta_0^2 \rangle = \frac{2k_B T}{VB\epsilon_c(1-\sigma)}, \quad (15)$$

where k_B is the Boltzmann constant. As the system approaches the chevron transition, chevronlike fluctuations grow, and their magnitude diverges at the transition.

This eigenmode corresponding to the largest eigenvalue destabilizes the uniform structure with respect to the chevron. The new nascent chevron structure is more sinelike in the region where the leading eigenvalue is small and positive. The amplitude θ_0 in this region may be estimated by adding the effect of the quartic term in θ due to this mode alone to Eq. (7). For further discussion, the reader is referred to the papers by Limat and Prost [5], and by Kralj and one of the present authors [6].

III. HYDRODYNAMIC EQUATIONS

A. Basic equations

We use a hydrodynamic formulation in terms of the displacement $u(\mathbf{r}, t)$. The advantage of this formulation is that it includes both layer compressibility and layer bending on an equal footing. We follow the exposition of the hydrodynamic equations for Sm-A by Chaikin and Lubensky [10,12]. We modify their formulation by including terms in the free energy that allow for the chevron tip. The important point is that the layer displacement u is the only nonstandard hydrodynamic variable, to which we must add the local fluid velocity \mathbf{v} . We suppose the fluid to be incompressible, and the temperature to be constant; these assumptions are not crucial, but considerably simplify calculations.

The equation for the displacement is

$$\frac{\partial u}{\partial t} - v_3 = \lambda_p \nabla \cdot \mathbf{J}, \quad (16)$$

where

$$J_i = \frac{\delta F}{\delta \partial_i u}. \quad (17)$$

The coefficient λ_p is the usual permeation constant of Sm-A hydrodynamics [9], which relates the layer flux through a stationary medium to the relevant thermodynamic force. Using Eq. (5) one obtains

$$J_i = \delta_{ix} [B(\frac{1}{2}u_x^2 - \epsilon)u_x - Ku_{xxx}]. \quad (18)$$

The momentum density $\varrho \mathbf{v}$ obeys the equation

$$\frac{\partial}{\partial t}(\rho v_i) = \frac{\partial \sigma_{ij}}{\partial x_j}. \quad (19)$$

The stress tensor σ_{ij} is given by

$$\sigma_{ij} = -p \delta_{ij} - \varrho v_i v_j + \delta_{i3} J_j + \sigma'_{ij}, \quad (20)$$

where p is the pressure (which we shall suppose uniform) and σ'_{ij} is the dissipative part of the strain tensor

$$\sigma'_{ij} = \eta_{ijkl} \partial_k v_l. \quad (21)$$

The viscosity tensor [12] takes the form

$$\begin{aligned} \eta_{iklm} = & \eta_1 a_i a_k a_l a_m + \eta_2 (\delta_{il}^\perp \delta_{km}^\perp + \delta_{kl}^\perp \delta_{im}^\perp) + (\eta_4 - \eta_2) \delta_{ik}^\perp \delta_{lm}^\perp \\ & + \eta_3 (a_i a_l \delta_{km}^\perp + a_k a_l \delta_{im}^\perp + a_i a_m \delta_{kl}^\perp + a_k a_m \delta_{il}^\perp) \\ & + \eta_5 (a_i a_k \delta_{lm}^\perp + a_l a_m \delta_{ik}^\perp). \end{aligned} \quad (22)$$

In these equations, the quantity \mathbf{a} takes its conventional meaning of a unit vector normal to the layers, and

$$\delta_{ik}^\perp = \delta_{ik} - a_i a_k.$$

Equations (16,19) can be further simplified by using the incompressibility condition, $\nabla \cdot \mathbf{v} = 0$. Firstly, if the only geometrical symmetry of the system that is violated is that which gives rise to the chevron mode, then $v_y = v_2 = 0$. Secondly, we may observe that for a perturbation homogeneous in the plane of the cell,

$$v_z(x, z, t) = v_3(x, z, t) = v_3(x, t), \quad (23)$$

and thus

$$\frac{\partial v_3}{\partial z} = 0. \quad (24)$$

The incompressibility condition can be expressed as

$$\nabla \cdot \mathbf{v} = \frac{\partial v_1}{\partial x} + \frac{\partial v_3}{\partial z} = 0. \quad (25)$$

Thus

$$\frac{\partial v_1}{\partial x} = 0. \quad (26)$$

We now further suppose homogeneity in the z direction for v_1 , then $v_1(x, z, t) = v_1(x, t)$. This condition is equivalent to a statement that there are no convection-induced rolls. Now the only consistent solution for v_1 is $v_1 = 0$. Thus the velocity has only one nonzero component $v_3(\mathbf{r}, t) = v_3(x, t)$.

As a result of these simplifications, the governing equations (16,19) now reduce to

$$\frac{\partial u}{\partial t} - v_3 = \lambda_p h, \quad (27a)$$

$$\varrho \frac{\partial v_3}{\partial t} - \eta_3 \partial_x^2 v_3 = h, \quad (27b)$$

where

$$h = \nabla \cdot \mathbf{J} = B \partial_x [(\frac{1}{2}u_x^2 - \epsilon)u_x] - Ku_{xxxx} \quad (28)$$

is the variable conjugate to the smectic displacement u .

We now apply nonslip and strong (angular) anchoring boundary conditions for the displacement u ,

$$u(\pm L/2, t) = 0, \quad (29a)$$

$$u_x(\pm L/2, t) = \theta(\pm L/2, t) = 0, \quad (29b)$$

and finally apply nonslip boundary conditions for the velocity:

$$v_3(\pm L/2, t) = 0. \quad (29c)$$

Equations (27a,27b) together with the boundary conditions (29a,29b,29c) describe the process of chevron structure formation. However, the real process depends strongly on the boundary conditions at the edges of the cell.

One can imagine two possible scenarios. If the ends of the cell are open, then liquid moves almost freely along the substrates. As the layers start bending they provoke mass flow, and this hydrodynamical coupling is a crucial component in the layer motion. In this case both Eqs. (27a) and (27b) are required for a correct description.

If, by contrast, the ends of the cell are closed and are, for example, under pressure, the situation is different. In this circumstance, there is no room in the cell for the liquid to move. Now there is no longer any mass flow, and chevron formation is due to layer permeation through the stationary liquid alone. The molecules rearrange themselves forming new layers during this process. Only Eq. (27a) is required. The hydrodynamic velocity, and the equation governing it, are suppressed.

Although these two processes are, of course, described by the same set of hydrodynamic equations, they differ from each qualitatively. In this paper, we restrict ourselves only to the former scenario. We shall discuss the latter scenario elsewhere.

B. Nondimensionalization

1. Time scales

We first note that there are in fact no fewer than *three* characteristic time scales for the hydrodynamics of a smectic-A liquid crystal. These are

$$\tau_p = \frac{L^4}{4\pi^2 K \lambda_p}, \quad (30)$$

$$\tau_i = \frac{\rho L^2}{4\pi^2 \eta_3}, \quad (31)$$

$$\tau_v = \frac{\eta_3 L^2}{4\pi^2 K}, \quad (32)$$

with

$$\tau_p \gg \tau_v \gg \tau_i. \quad (33)$$

The permeation process by itself takes place on time scales $\sim \tau_p$. This would be the only relevant time scale if mass flow were forbidden and is the longest of the three time scales. The time scale τ_i is the time scale required for viscous forces to respond to the inertia. This motion is sometimes known in the literature as the *fast mode* [9]. This time scale is the shortest of the three. Finally the time scale τ_v , which will turn out to be the relevant time scale in this study, comes from a balance between the viscous and the elastic forces. This is sometimes known in the literature as the *slow mode* [9], though we caution the reader that of the three time scales, it is in fact the intermediate!

The quantity τ_v can also be expressed in terms of the critical strain

$$\tau_v = \eta_3 / B \epsilon_c. \quad (34)$$

The three time scales can be reinterpreted in terms of a fundamental time scale τ_v , with, in addition, two small parameters related to the ratios between them. The small parameters are

$$\delta_1 = \frac{4\pi^2 \tau_i}{\tau_v} = \frac{4\pi^2 K \rho}{\eta_3^2}, \quad (35)$$

$$\delta_2 = \frac{\tau_v}{\tau_p} = \frac{\eta_3 \lambda_p}{L^2}. \quad (36)$$

The order of magnitude of these δ_1 and δ_2 can be estimated as follows. Assuming $\eta_3 = 1$ poise, $K = 10^{-6}$ dyn, and $\rho = 1$ gm cm $^{-3}$ we estimate $\delta_1 \sim 10^{-5}$. To estimate δ_2 , we take $\lambda_p \eta_3 = 10^{-14}$ cm 2 [9], $L = 10^{-3}$ cm, obtaining $\delta_2 \sim 10^{-8}$. Values of $K = 10^{-6}$ dyne, $L = 10^{-3}$ cm, $\eta_3 = 1$ poise, yield $\tau_v \approx 10^{-2}$ s. In contrast, $\tau_p \sim 10^6$ s ~ 12 days.

2. Scaling the equations

As indicated above, we choose to scale time with respect to τ_v . We use the following dimensionless variables:

$$\tilde{x} = \frac{x}{L}, \quad (37a)$$

$$\tilde{t} = \frac{t}{\tau_v}, \quad (37b)$$

$$U(\tilde{x}, \tilde{t}) = \frac{u(x, t)}{L\sqrt{2\epsilon_c}}, \quad (37c)$$

$$V(\tilde{x}, \tilde{t}) = \frac{t_{sc}}{L\sqrt{2\epsilon_c}} v(x, t), \quad (37d)$$

$$\vartheta(\tilde{x}, \tilde{t}) = \frac{\theta(x, t)}{\sqrt{2\epsilon_c}} = U_{\tilde{x}}(\tilde{x}, \tilde{t}). \quad (37e)$$

We have added to the hydrodynamic variables a scaled angular variable ϑ . This refers to the layer tilt. We have seen in Eq. (5) that the static chevron properties are most conveniently computed in terms of these angular variables. Our choice of scaling the displacement is dictated by the stability analysis and guarantees U to be $O(1)$ for the chevron structure.

The nondimensionalized versions of Eqs. (27a) and (27b) are

$$U_{\tilde{t}} - V = \delta_2 H, \quad (38a)$$

$$\delta_1 V_{\tilde{t}} - V_{\tilde{x}\tilde{x}} = H, \quad (38b)$$

$$H = \frac{\partial}{\partial \tilde{x}} \left[(U_{\tilde{x}}^2 - \sigma) U_{\tilde{x}} - \frac{1}{4\pi^2} U_{\tilde{x}\tilde{x}\tilde{x}} \right]. \quad (38c)$$

The function H is a particularly important quantity in these equations. It is the scaled body force driving the motion of the system. It can be written as

$$H(\tilde{x}, \tilde{t}) = \frac{\partial}{\partial \tilde{x}} \frac{\delta \mathcal{F}}{\delta \vartheta}, \quad (39)$$

where \mathcal{F} is nondimensionless version of Eq. (1), defined by

$$\mathcal{F} = \frac{1}{2} \int_{-1/2}^{1/2} d\tilde{x} \left[\frac{1}{2} (\sigma - \vartheta^2)^2 + \frac{1}{4\pi^2} \vartheta_{\tilde{x}}^2 \right]. \quad (40)$$

The scaling of the functions U , V , H requires that these quantities and their derivatives are $O(1)$. We can conclude that the body force does affect the system on this time scale. In contrast, chevron formation on time scale τ_p will be considered elsewhere [16].

3. Solving the governing equations

A full treatment involves multitime scale analysis [13]. The solution to Eqs. (38a, 38b) can formally be written as

$$U(\tilde{x}, \tilde{t}) = U^{(0)}(\tilde{x}, \tilde{t}) + o(\delta_1, \delta_2), \quad (41)$$

$$V(\tilde{x}, \tilde{t}) = V^{(0)}(\tilde{x}, \tilde{t}) + o(\delta_1, \delta_2). \quad (42)$$

The dominant behavior is given by $U^{(0)}$ and $V^{(0)}$. The hierarchy of time scales makes the inertia and permeation terms negligible. Because of the large viscosity and very long permeation time, chevron formation is governed by a balance between the body and viscosity forces. We shall take into account only these lowest-order terms. We shall simplify notation by suppressing the superscripts at this stage (we shall restore the original variables later). Relatively simple analysis of Eqs. (38a, 38b) now yields

$$V(\tilde{x}, \tilde{t}) = U_{\tilde{t}}(\tilde{x}, \tilde{t}), \quad (43a)$$

$$V_{xx}^- = -H = -\frac{\partial}{\partial \tilde{x}} \frac{\delta \mathcal{F}}{\delta \vartheta}. \quad (43b)$$

It turns out that this pair of equations is now more conveniently reexpressed in angular variables. From Eq. (43a), we have

$$V_{xx}^- = U_{txx}^-, \quad (44)$$

which may be more conveniently reexpressed in terms of $\tilde{\vartheta}$ using its definition, Eq. (37e):

$$V_{xx}^- = \vartheta_{xt}^-. \quad (45)$$

Now combining Eqs. (43b) and (45), we obtain

$$\frac{\partial}{\partial \tilde{x}} \left(\vartheta_t^- + \frac{\delta \mathcal{F}}{\delta \vartheta} \right) = 0. \quad (46)$$

We can now integrate this equation over \tilde{x} . The constant of integration is zero, from the reflection symmetry of ϑ . Thus the final governing equation is simply the time dependent Landau-Ginzburg equation, but now written in terms of ϑ :

$$\frac{\partial \vartheta}{\partial t} = -\frac{\delta \mathcal{F}}{\delta \vartheta}. \quad (47)$$

When the equation is written out in full, we obtain the well-known Fisher-Kolmogorov equation [14,15]:

$$\vartheta_t^- = (\sigma - \vartheta^2) \vartheta + \frac{1}{4\pi^2} \vartheta_{xx}^-. \quad (48)$$

It is useful as well to view this equation in our original notation:

$$\eta_3 \frac{\partial \theta}{\partial t} = -\frac{\delta F}{\delta \theta}, \quad (49)$$

where F is just the free energy proposed by Limat and Prost [5].

We now make some mathematical comments about the procedure. The original differential equations were first order in time, but *fourth* order in space. By redefining our variables, and performing one exact integration, we have been able to reduce the order of the differential equation. This does not, however, entirely come for free. The price we have paid is loss of information about layer slippage at the interfaces. Equivalently, the boundary condition $u(\pm L/2) = 0$ now becomes an *integral* condition on the solution $\vartheta(\tilde{x})$. The integral condition *restricts* the manifold of allowable solutions $\vartheta(\tilde{x})$.

Let us examine this point in more detail. In order to guarantee no layer slippage we require

$$\int_{-1/2}^{1/2} d\tilde{x} \vartheta(\tilde{x}, \tilde{t}) = \int_{-1/2}^{1/2} d\tilde{x} U_{\tilde{x}}^- = U(1/2) - U(-1/2) = 0. \quad (50)$$

The point is that this is not a local condition. In general it is very difficult to fulfill conditions of this type. Nevertheless, fortunately we can easily identify a (nonexhaustive!) set of solutions that does automatically satisfy the condition. This is the set of solutions that are odd with respect to $x \rightarrow -x$ inversion. This is in fact just the set of all chevronlike solutions. Other (nonodd) solutions that satisfy the integral condition are simply not considered.

The infinite anchoring boundary conditions are not affected by these considerations; however,

$$\vartheta(\pm 1/2, \tilde{t}) = 0. \quad (51)$$

IV. RESULTS

A. General considerations

We first make some general comments about the structure of the governing equation Eq. (48). As the chevron structure develops in time, the energy \mathcal{F} decays, approaching its global minimum in the final equilibrium state. In addition, the Euler-Lagrange equation of the functional \mathcal{F} possesses an exact integral,

$$I(\tilde{x}, \tilde{t}) = \frac{1}{2} (\sigma - \vartheta^2)^2 - \frac{1}{4\pi^2} \vartheta_x^2, \quad (52)$$

which approaches a constant value over the whole cell as the system approaches its final state. We can use this quantity to monitor the approach to equilibrium.

We now turn to the solution manifold. As we have indicated above, we may restrict our consideration to solutions odd in \tilde{x} . Any odd function can be expressed in terms of a Fourier series:

$$\vartheta(\tilde{x}, \tilde{t}) = \sum_{n=1}^{\infty} \vartheta_n(\tilde{t}) \sin(2\pi n \tilde{x}). \quad (53)$$

It will sometimes be useful to express $\vartheta(\tilde{x}, t)$ in terms of the time-dependent harmonic coefficients $\vartheta_n(\tilde{t})$.

In particular, in the initial stage of the chevron structure formation, when the book structure is quenched into an unstable state, one can obtain a linearized equation for $\{\vartheta_n(\tilde{t})\}$. In this limit, the modes are independent and their amplitudes either vanish identically or increase exponentially, each on their own characteristic time scale. However, at later times, the presence of nonlinear terms in ϑ^3 causes interaction between the modes, and the harmonic expansion is no longer as useful.

B. Near-critical strain

We first consider a regime close to the critical strain ϵ_c (σ is close to 1). In this regime the $\vartheta(\tilde{x}, t)$ is small at all times. We can now neglect the mode coupling and consider only the dominant mode in the Fourier expansion (53). This is the leading term in the expansion, and it develops faster than all the others. We do, however, need to include the nonlinear term in the equation, in order to avoid an unchecked expansion of the mode amplitude.

Thus in this limit we may take ϑ to be of the form

$$\vartheta(\tilde{x}, \tilde{t}) = \vartheta_1(\tilde{t}) \sin(2\pi\tilde{x}). \quad (54)$$

Multiplying Eq. (48) by $\sin(2\pi\tilde{x})$ and integrating over \tilde{x} we obtain a time-dependent Ginzburg-Landau equation for the amplitude ϑ_1 :

$$\frac{\partial \vartheta_1}{\partial \tilde{t}} = (\sigma - 1)\vartheta_1 - \frac{3}{4}\vartheta_1^3. \quad (55)$$

This is the generalization to the time domain of the analysis of the analogous statics in earlier work [6].

For strains less than the critical strain ($\sigma < 1$), fluctuations around the bookshelf geometry decay. The characteristic time scale is $t_v/(\sigma - 1)$. Thus, as might be expected, there is a critical slowing down in the decay rate as the critical strain is approached.

Above the critical strain, Eq. (55) has an analytical solution:

$$\vartheta_1(\tilde{t}) = \left(\frac{4(\sigma - 1)}{3} \right)^{1/2} \{1 + \exp[-2(\sigma - 1)(\tilde{t} - \tilde{t}_0)]\}^{-1/2}. \quad (56)$$

At early times the the solution exhibits exponential growth with characteristic time

$$t_c = t_v/(\sigma - 1) = \eta_3/B(\epsilon - \epsilon_c). \quad (57)$$

At late times ϑ_1 approaches $\sqrt{4(\sigma - 1)/3}$ exponentially. The angle θ and the layer displacement tend towards

$$\theta(x) = 2\sqrt{2(\epsilon - \epsilon_c)/3}\sin(2\pi x/L), \quad (58)$$

$$u(x) = L\sqrt{2(\epsilon - \epsilon_c)/3\pi^2}(1 + \cos(2\pi x/L)).$$

The characteristic times associated with approach to equilibrium are smaller than those associated with growth by a factor of 2. Both these times, therefore, exhibit critical slowing down, associated with the disappearance of the equilibrium amplitude.

C. Beyond the critical régime

For $|\sigma - 1|$ no longer very small, the interaction between harmonics can no longer be neglected. We have been unable to find an analytic solution. However, the problem has been solved in a straightforward way numerically using both real space and spectral methods. We start typically with a small displacement corresponding to the first harmonic. However, the initial conditions are not important, because the $\vartheta_1(\tilde{t})$ increases more rapidly than other harmonics. Low-level white noise initial conditions gives essentially the same results. We are able to verify that the equilibrium solution is reached consistently in two ways. First we monitor the free energy F , which decreases monotonically with time, as it should. Second we monitor the behavior of the integral $I(\tilde{x}, \tilde{t})$ defined in Eq. (52), which tends to a constant as equilibrium is approached. This latter method also serves as an automatic check on the accuracy of the numerical scheme.

We can discern a number of common features in the results. The characteristic time seems to be $\tau_v/(\sigma - 1)$, as might be expected by extrapolating analytically from the

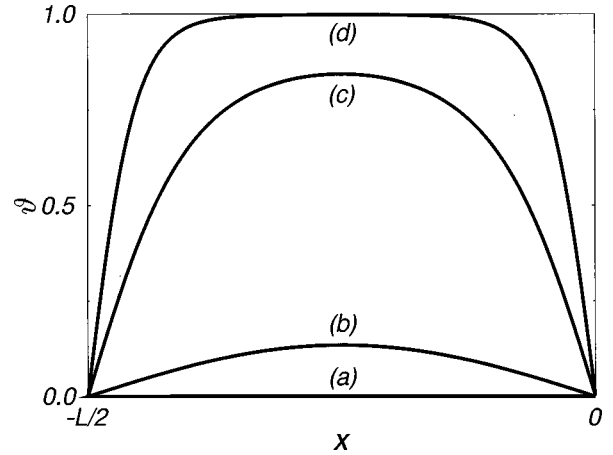


FIG. 2. Growth of chevron tilt angle as a function of scaled time over half the cell ($-L/2 \leq x \leq 0$) for $\sigma = 25.0$. Curve *a* is the initial condition, with very small fluctuation. Curves *b*, *c*, and *d* are curves at later times $\tilde{t} = 1, 2, 3$, respectively. The other half-cell exhibits the same behavior with opposite sign. Note how the sinusoidal shape at early times is replaced by a flat-topped structure at late times.

critical régime. In all cases the amplitude of the lowest harmonic increases until the layer tilt at $\pm L/4$ reaches the value of $\sqrt{2}\epsilon$. This is the value at which layer tilt just compensates for the surface-induced layer mismatch. This tilt region then expands until it encompasses the whole layer, apart from small regions of size of the healing length at the chevron tip and close to the walls. This is just the length required for layer reorientation enforced by the boundary conditions. A typical example of this behavior is shown in Fig. 2. We here concentrate on angular rather than displacement variable because this particular physical feature is most clearly illustrated in this way. In Fig. 3 the same information is presented, now concentrating on the chevron displacement $u(x, t)$. The sharply peaked chevron only develops at late times.

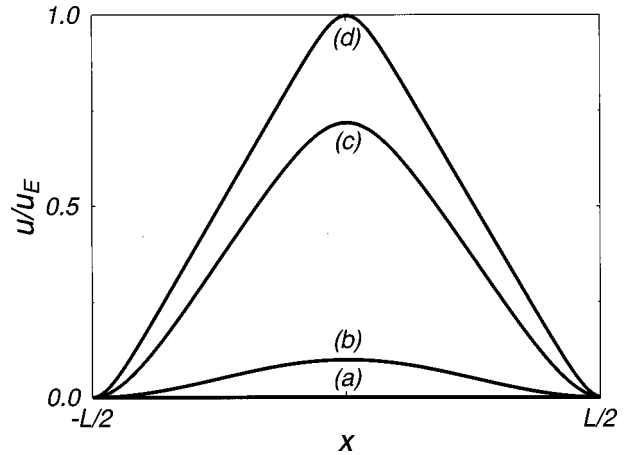


FIG. 3. Same as previous figure, but now showing chevron displacement as a function of time, normalized so that the chevron tip displacement is unity at equilibrium. In this set of curves $\sigma = 25.0$. Curves *a*–*d* have the same significance as in the previous figure. In these curves, the sinusoidal shape at early times is replaced by the sharply peaked classical chevron structure at late times.

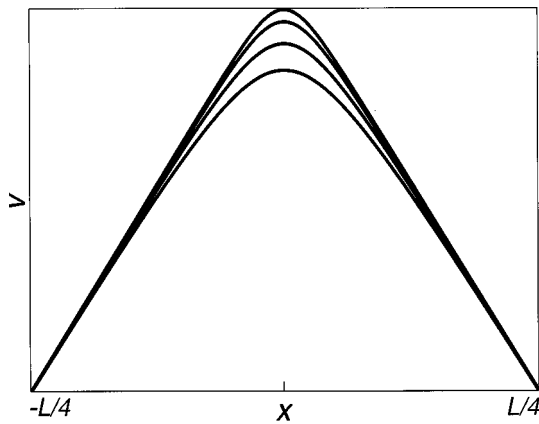


FIG. 4. Normalized displacement v at the chevron tip, at late times for $\sigma=625$. Higher curves are for later times. The chevron structures have been displaced in such a way that the arms of the chevron lie on top of each other. There is also a secular motion of these arms resulting from tightening of the curvature of the layers near $x=\pm(L/2)$. The superposition of the arms highlights the decreasing chevron tip thickness overlying an otherwise time-independent structure.

An equivalent way of looking at the the layer displacement involves the thickness of the chevron tip. The late time relaxation process in the high σ limit *sharpens* the chevron tip. We show this phenomenon qualitatively in in Fig. 4. In this figure we see the shape of the tip sharpen up in the limit of late times. In Fig. 5 we follow quantitatively the width of the the chevron tip as a function of time for a typical case.

We now try to draw together results for the whole range of σ . The characteristic time $\tau_v/(\sigma-1)$ seems to govern the shape of the relaxation process. In Fig. 6 we show the time dependence of the maximum displacement, normalised to its final value, for several different σ , in all cases plotted in terms of the relevant characteristic time. It will be observed that the curves almost collapse on to one universal curve, with the low σ and high σ curves differing slightly. This latter effect is expected, as the low σ case is dominated by a single harmonic, whereas the high σ case is more complex.

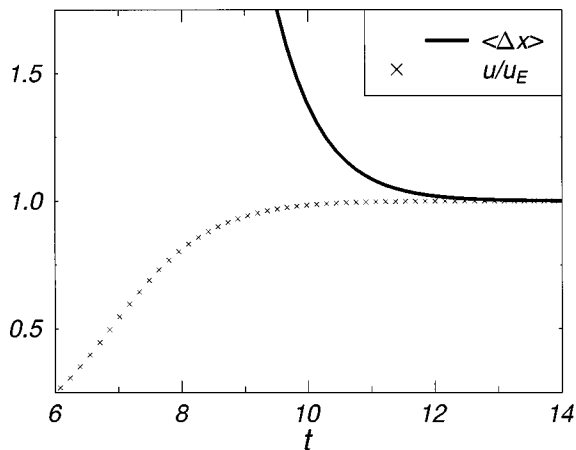


FIG. 5. Time dependence of the normalized displacement $u(x)/u_E$ and the normalized width $\langle \Delta x \rangle$ of the chevron tip, as a function of scaled time, for $\sigma=625$. The quantity $(d\theta/dx)_{x=0}^{-1}$ is taken as a measure of the width.

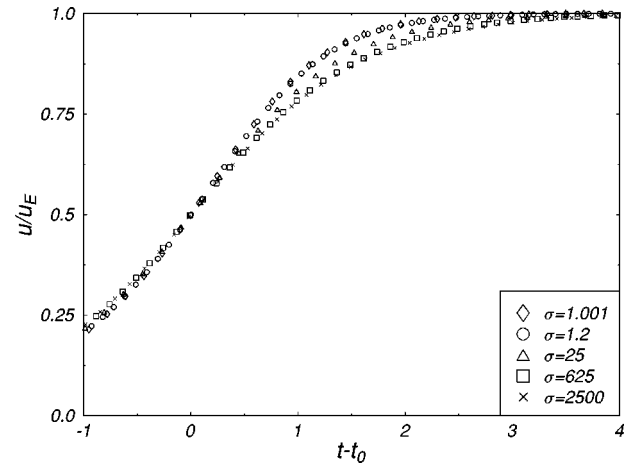


FIG. 6. Scaled time dependence of the maximum normalized displacement $u(0)/u_E$, for various σ . The curves are very close together, and reduce to one universal curve at low times. At late times, two universal limits, at low and high σ , are easily discernible.

V. SUMMARY AND CONCLUSIONS

In this paper we have examined the process which occurs when a Sm-A in a bookshelf structure within a cell is quenched into a state in which it is no longer stable and the layers buckle. What follows is the evolution of the so-called chevron structure, and this study has been concerned with the dynamics of the chevron evolution. The motivation, of course, is not so much the Sm-A phase itself, in which the chevron is an interesting but ultimately useless phenomenon, but the possible application to the Sm-C phase. In this latter case there is an analogous phenomenon whose properties are of vital technological concern for ferroelectric display technology. This study involves a toy model, the real worth of which will eventually be judged by whether or not it turns out to be possible to extend this work to study switching in Sm-C cells containing chevron defects.

The driving force for this phenomenon is the mismatch between the layer spacings in the bulk and at the interfaces. It is extremely sensitive to the boundary conditions on the surfaces of the cell. The natural expression for the free energy involves the layer displacement from the bookshelf geometry. Interestingly, the statics is most easily solved by transforming from displacement to angular variables, where the local angle describes the orientation of the layer with respect to the bookshelf geometry [5,6]. The statics is governed by a non-dimensionalised layer strain, which we have labeled [6] as the chevron number, which is unity at the onset of the deformation.

Our analysis of the dynamical problem supposes that the system is quenched so that the bulk-surface mismatch suddenly appears, essentially on zero time scale. We have derived the resulting hydrodynamical equations, which strongly couple layer displacement and hydrodynamical velocity. The layer displacement is actually a replacement of the more general layer phase, which is a conserved quantity. The result is that the governing equations appear quite complex. The layer displacement is driven not only by a free energy-related driving force but also by the hydrodynamical velocity. The latter is dominant, but even the former involves a gradient of the

nonequilibrium current, rather than the current itself.

There are three possible relaxation times in the problem, roughly speaking on time scales of nanoseconds, milliseconds, and hours. The relaxation seems to be dominated by the intermediate of these, which we have labelled the viscous relaxation time. From a mathematical point of view, the interesting feature is that a complex coupled problem can be transformed to a simple time dependent Ginzburg-Landau problem by using the angular variable rather than the displacement as the principal quantity. What results is the Fisher-Kolmogorov equation, though in practice the most interesting property of this equation—that it can sustain a traveling wave—does not seem to play a role.

The effect of this is that the problem can be almost but not entirely nondimensionalized, dominated by a time scale that is essentially the viscous relaxation time divided by the chevron number (less one close to the onset of the chevron behavior). Quantitatively, we remark on the critical slowing down phenomenon in the near-critical regime. Qualitatively, we note slight differences between the time dependence of the near-critical behavior, for which the deformation is sine-wave-like, and well-developed deformations, for which the deformation is V shaped. Essentially, however, the maximum displacement obeys a tanh-like structure (though notably *not* exactly a tanh) as a function of time. The initial stage of the process is the growth of the principal harmonic. At later stages, for σ large enough, the other harmonics kick in in such a way as to transform the sine wave into a V shape. The final stage can be thought of as the sharpening of the chevron tip between the two opposite layer orientations.

The problem in observing this phenomenon is twofold. The dominant time scale $\sim 10^{-2}$ sec requires that the quenching process be quicker than that. This seems a tall order. However, if the quench is in to a region just beyond the chevron onset the quench time scales become shorter and the relaxation times get longer, so this must be the area in which experiments are first attempted.

A second complication concerns the ability of the system to sustain hydrodynamics flows at all. The suspicion must be that if the cell is closed at the ends, rather than open, the no-slip velocity boundary conditions will strongly inhibit the hydrodynamic flows that we find to dominate the chevron relaxation process. This will suppress entirely the hydrody-

amic coupling, and restore the order parameter relaxation process. This is the permeation process in which the layers pass through the fluid. From a physical point of view, the coupling of hydrodynamical velocity to the order parameter motion has accelerated the relaxation from a time scale of hours to a time scale of milliseconds.

We shall find that the properties of the relaxation process found in the present study are considerably simpler, both from a mathematical and a physical point of view, than those predicted in the permeation case. We postpone, however, the description of this phenomenon to the next paper in this series.

We can remark, however, that at the surfaces of the cell, the velocity no-slip boundary condition slows down surface relaxation; at the surface only permeation can occur. In this study we have restrained *entirely* layer slippage at the surface, and attributed this to a molecular *Deus ex machina* which somehow obtains a memory of the surface layering. Relaxing the layer boundary condition to allow surface permeation, however, would not have made any difference to this conclusion, because we have taken the limit $\delta_2 \rightarrow 0$, which is equivalent to the limit $\tau_p \rightarrow \infty$.

Thus the strong implication of this study, to be confirmed in later more detailed investigations, is that the formation of chevrons does not necessarily provide evidence for surface memory effects. Rather it arises from a competition between slow permeation, which would lead to layer slippage, tilted layers and a true energy minimum, and rapid layer buckling leading to a metastable chevron. We use the term buckling advisedly. The thrust of our argument is that the chevron structure is but one of a large class of buckling phenomena, of which the classical paradigm occurs in beams [17]. In all such phenomena, the pain of microscopic compression is avoided by, albeit inhomogeneous, macroscopic reorientation.

ACKNOWLEDGMENTS

A.N.S. is grateful to EPSRC and INTAS for financial support in Southampton and St. Petersburg. L.D.H. is grateful to EPSRC and DERA, Malvern for a CASE studentship, T.J.S. is grateful to S. Kralj, N. Vaupotič, G. Durand, S. Zumer, A.A. Wheeler, as well as members of the British Smectic C Consortium, for useful discussions.

-
- [1] T. P. Rieker, N. A. Clarke, G. S. Smith, D. S. Parmar, E. B. Sirota, and C. R. Safinya, *Phys. Rev. Lett.* **59**, 2658 (1987).
- [2] For some relevant theoretical work on the chevron structure in the Smectic C^* phase, see e.g.: M. Nakagawa, *J. Phys. Soc. Jpn.* **59**, 1995 (1990); S. Ukai and M. Nagakawa, *ibid.* **61**, 112 (1992); S. Ukai and M. Nagakawa, *ibid.* **62**, 1984 (1993); L. Limat, *J. Phys. II* **5**, 803 (1995); W. J. Hartmann and A. M. Luyckxsmolders, *J. Appl. Phys.* **67**, 1253 (1990); L. Le Bourhis and L. Dupont, *Mol. Cryst. Liq. Cryst.* **275**, 155 (1996); N. Vaupotič, S. Kralj, M. Čopič, and T. J. Sluckin, *Phys. Rev. E* **54**, 3783 (1996); N. Vaupotič, M. Čopič, and T. J. Sluckin, *ibid.* **57**, 5651 (1998).
- [3] H. Takazoe, T. Toyooka, J. Horakata, and A. Fukuda, *Jpn. J. Appl. Phys., Part 1* **26**, L240 (1987).
- [4] Y. Ouchi, Y. Takanishi, H. Takazoe, and A. Fukuda, *Jpn. J. Appl. Phys., Part 1* **28**, 2547 (1989).
- [5] L. Limat and J. Prost, *Liq. Cryst.* **13**, 101 (1993).
- [6] S. Kralj and T. J. Sluckin, *Phys. Rev. E* **50**, 2940 (1994).
- [7] M. Nakagawa and T. Akahane, *J. Phys. Soc. Jpn.* **55**, 1516 (1986).
- [8] M. Cagnon and G. Durand, *Phys. Rev. Lett.* **70**, 2742 (1993).
- [9] P. G. de Gennes and J. Prost, *The Physics of Liquid Crystals* 2nd ed. (Clarendon Press, Oxford, 1993).
- [10] P. M. Chaikin and T. C. Lubensky *Principles of Condensed Matter Physics* (Cambridge University Press, New York, 1995).
- [11] M. Delaye and P. Keller, *Phys. Rev. Lett.* **37**, 1065 (1976).
- [12] There are a number of related expositions of smectic-A hydro-

- dynamics in the literature. That cited most often in the western literature is that due to P. C. Martin, O. Parodi, and P. S. Pershan, Phys. Rev. B **6**, 2401 (1972); A Poisson bracket formulation which gives the same linear response limit has been written down by: E. I. Kats and V. V. Lebedev, *Fluctuation Effects in the Dynamics of Liquid Crystals* (Springer-Verlag, Berlin, 1994).
- [13] C. M. Bender and S. A. Orszag, *Advanced Mathematical Methods for Scientists and Engineers* (McGraw-Hill, London, 1987)
- [14] D. Zwillinger, *Handbook of Differential Equations* (Academic Press, London, 1992).
- [15] See, e.g., W. van Saarloos, Phys. Rev. A **37**, 211 (1988); This equation, now almost ubiquitous in various branches of applied mathematics and theoretical physics, has a long and distinguished history. It is referred to as the modified Fisher equation in [14]. The Fisher in question is not M. E. Fisher (as one would normally expect in theoretical physics!) but the distinguished geneticist and statistician R.A. (Sir Ronald) Fisher. The equation has acquired his sobriquet following his paper R. A. Fisher, Ann. Eugenics **7**, 355 (1937).
- [16] A. N. Shalaginov, T. J. Sluckin, and L. D. Hazelwood (unpublished).
- [17] Analogous buckling phenomena occur when the layers are in the plane of the cell, rather than perpendicular to it. This occurs even without any surface memory effect! The threshold process is usually known as the Helfrich-Hurault instability. See W. Helfrich, Appl. Phys. Lett. **17**, 531 (1970); J. P. Hurault, J. Chem. Phys. **59**, 2086 (1973); The deformations themselves, which can be generated either by explicit compression, or simply by changing the temperature, were first observed by: M. Delaye, R. Ribotta, and G. Durand, Phys. Lett. A **44**, 139 (1973).